Identifying Orbit Lengths for Promotion

Elise Catania[a] Jack Kendrick[b] Heather M. Russell[c]
Julianna Tymoczko[d]

Submitted: Dec 14, 2025; Accepted: May 7, 2026; Published: Aug 28, 2026

Abstract

In this work we study Schützenberger's promotion operator on standard Young tableaux via a corresponding graphical construction known as $m-$diagrams. In particular, we prove that certain internal structures of SYT are preserved under promotion and correspond to distinct components of $m-$diagrams. By treating these structures as atomic parts of the $m-$diagram, we provide a simple algorithm for computing the promotion orbit length of rectangular SYT. We conclude the paper by applying our results to (column) semi-standard Young tableaux and prove a formula for the promotion orbit lengths of rectangular (column) SSYT.

Mathematics Subject Classifications: 05E10, 05C10

1 Introduction

Young tableaux are fundamental combinatorial objects. With various choices of fillings and rules for manipulations, Young tableaux encode important data and processes from across mathematics [4]. We focus on Schützenberger's *promotion* operator on *standard Young tableaux* [19]. Promotion features in the study of representations and algebraic operations on representations [1, 6, 9, 13, 27], Schubert varieties and the cohomology ring structure induced by Schubert classes [24, 25], and other constructions in algebra and geometry [3, 11]. The promotion map acts bijectively on the set of standard Young tableaux of a fixed shape so it is reasonable to ask about the orbits of this map.

Initial results in this area address the natural question of whether the size of an orbit can be determined from only one representative tableau. The *promotion order* of the shape λ is the minimum N such that $P^N(T) = T$ for every tableaux T of shape λ. In

[a] School of Mathematics, University of Minnesota, Minneapolis, MN (`catan042@umn.edu`).
[b] Cancer Research UK Cambridge Institute, University of Cambridge, Cambridge, UK (`jack.kendrick@cruk.cam.ac.uk`).
[c] Department of Mathematics and Statistics, University of Richmond, Richmond, VA `hrussell@richmond.edu`).
[d] Department of Mathematics and Statistics, Smith College, Northampton, MA (`jtymoczko@smith.edu`).

general, the promotion order is not well-behaved. For instance, the promotion order of the shape $\lambda = (8, 6) \vdash 14$ is 7,554,844,752 [21]. Seminal — and very surprising — work of Haiman shows that when we restrict to $m \times n$ *rectangular* standard Young tableaux, the order of promotion is mn [6]. Haiman in fact completely characterizes all shapes λ such that the order of promotion is $|\lambda|$, showing that their constituent pieces are rectangles and variations of what he calls staircases. Subsequent work has focused on rectangles. Rhoades used cyclic-sieving phenomena to obtain data about the structure and sizes of promotion orbits, showing that the number of rectangular tableaux fixed by n applications of the promotion operator is measured by the quantum hook-length polynomial [15, 16]. This has been explored and extended in different contexts, using related operators [10, 22, 23] or equivariant maps to other sets of objects equipped with a cyclic group action [2, 12, 17, 26].

Yet, little has been done to analyze the sizes and elements of promotion orbits for *specific* standard Young tableaux, despite analogous classification and stability questions in representation theory. The only exception we found is a bijection between the set of rectangular tableaux in minimal promotion orbits and the symmetric group in the number of columns, due to Purbhoo and Rhee [14].

In this paper, we give a process for computing the size of a rectangular tableau's promotion orbit by exploiting the geometry of an object called an $m-$diagram. An $m-$diagram is a union of noncrossing matchings; the connected components of an $m-$ diagram refine the data of a noncrossing partition. While promotion of rectangular tableaux is not equivariant with rotation of $m-$diagrams, we show that the $m-$diagrams nonetheless encode important information. In particular, we do the following:

1. Define a notion of uniformly equivalent tableaux and investigate promotion via the graphical construction of $m-$diagrams.

2. Provide an algorithm to determine the orbit length of a tableau based on geometric symmetries of the connected components in its corresponding $m-$diagram. In particular, this allows us to analyze orbit lengths when the $m-$diagrams are disconnected (see Theorem 25).

3. Extend our ideas to (column) semi-standard Young tableaux and provide a formula for the orbit lengths of these tableaux.

Our use of $m-$diagrams is motivated by their role as the intermediate step in constructing a kind of planar graph called a *web graph* [26]. Web graphs are the morphisms in a diagrammatic version of the representation category for $U_q(\mathfrak{sl}_n)$ and can be used to construct $U_q(\mathfrak{sl}_n)$-invariant vectors [8]. The number of $m \times n$ standard tableaux turns out to count the size of a basis for $U_q(\mathfrak{sl}_n)$-invariant vectors with mn tensor factors [7]. When $n = 2$ or $n = 3$, the natural bijection between $m \times n$ standard tableaux and web graphs is equivariant with respect to promotion and rotation, in the sense that the web corresponding to the promotion of T can be obtained from the web corresponding to T by rotating [12]. For larger n, identifying web bases that preserve this equivariance with respect to promotion and rotation is an active area of research; recent work of Gaetz et alia proposes one such basis for $n = 4$ [5]. The $m-$diagrams used in this paper are monochrome versions of a stranding that appears in [18] as the intermediate step in constructing a basis of $\mathfrak{sl}_n$ web graphs. In short, both the general question of understanding promotion orbits of tableaux and the specific graph construction of $m-$diagrams are important in representation theory and knot theory. However, this technical context is unnecessary in the paper at hand, so we omit it in what follows.

In addition, our paper does not examine the structure of $m-$diagrams in great detail. We leave as an open question whether sharper analysis would give more information about promotion orbits.

Outline

In Section 2 we provide the necessary background on standard Young tableaux and $m-$diagrams. Our main results on the promotion orbit lengths of rectangular SYT are contained in Section 3. We conclude the paper by applying our results to (column) semi-standard Young tableaux in Section 4.

2 Preliminaries

2.1 Tableaux

We begin by fixing notations and conventions for tableaux.

Definition 1 (Standard Young Tableau)**.** Suppose $\lambda = (\lambda_1 \geqslant \lambda_2 \geqslant \cdots \geqslant \lambda_k)$ is a partition of n. A *Young diagram* of shape λ is a grid of left- and top-aligned boxes with λ_i boxes in the i^{th} row for each $1 \leqslant i \leqslant k$. If all parts of the partition λ are the same then we call λ a rectangular partition and its Young diagram a *rectangular Young diagram.*

A *standard Young tableau (SYT)* is a filling of the Young diagram for λ with values $1, \ldots, n$ without repetition such that rows strictly increase left-to-right and columns strictly increase top-to-bottom. The *content* of a tableau T is the collection of integers filling its boxes.

Given two partitions μ and λ with $\mu_i \leqslant \lambda_i$ for all i, the set of boxes belonging to the Young diagram corresponding to shape λ but not μ yields a *skew diagram* of shape λ/μ. A *skew tableau* is a filling of a skew diagram such that for each box, all entries to the right and below are strictly larger.

Given a tableau T, we denote the number of boxes in T as $|T|$ and the entry in the i^{th} row and j^{th} column of T as T_{ij}. Next, we review Schützenberger's jeu de taquin promotion on SYT, which is a function from SYT of fixed shape λ to SYT of the same shape [19, 20].

Definition 2 (Promotion)**.** Given an SYT T, the *promotion* of T is the SYT $P(T)$ created as follows:

1. Erase 1 in the top left corner of T and leave an empty box.

2. Given the configuration $\begin{array}{|c|c|}\hline & b \\ \hline a \\ \cline{1-1}\end{array}$ and $b < a$ then slide b left; else if $a < b$ slide a up.

3. Repeat the above process until there are no nonempty boxes below or to the right of the empty box.

4. Decrement all entries by 1 and insert the largest entry of T into the empty box.

Example 3. Figure 1 gives an example of an SYT T and its promotion $P(T)$. This tableau will serve as our running example.

$$T = \begin{array}{|c|c|c|c|c|c|}\hline 1 & 2 & 6 & 7 & 14 & 19 \\ \hline 3 & 8 & 9 & 15 & 18 & 21 \\ \hline 4 & 10 & 11 & 16 & 20 & 23 \\ \hline 5 & 12 & 13 & 17 & 22 & 24 \\ \hline \end{array} \longrightarrow \begin{array}{|c|c|c|c|c|c|}\hline 1 & 5 & 6 & 13 & 17 & 18 \\ \hline 2 & 7 & 8 & 14 & 19 & 20 \\ \hline 3 & 9 & 10 & 15 & 21 & 22 \\ \hline 4 & 11 & 12 & 16 & 23 & 24 \\ \hline \end{array} = P(T)$$

Figure 1: The tableau T and its promotion $P(T)$

We are particularly interested in the orbits of tableaux under promotion. For a given SYT T, we denote the promotion orbit of T by $\mathcal{O}(T)$. The key observation in our approach is that certain internal structures of SYT are preserved during promotion. To this end, we introduce the following definition.

Definition 4 (Equivalence)**.** Suppose S and T are skew tableaux with $|S| = |T|$ and contents $\{s_1, s_2, \dots, s_n\}, \{t_1, t_2, \dots, t_n\}$. We say that S is *equivalent* to T, or $S \equiv T$, if S and T are the same after each tableau is left justified with the entries relabeled smallest to largest so that the content becomes $\{1, 2, \dots, n\}$. Moreover, we say S is *uniformly equivalent* to T if the content of S is $\{k + i_1, k + i_2, \dots, k + i_n\}$ and the content of T is $\{\ell + i_1, \ell + i_2, \dots, \ell + i_n\}$ for some k, ℓ and $S \equiv T$.

Remark 5. Note that if $i_1, \dots, i_n$ is equal to $1, \dots, n$ and S, T are not skew, then S and T are uniformly equivalent to an SYT.

Uniform equivalence is a powerful condition that allows us to treat uniformly proper sub-tableaux as atomic parts of the corresponding m-diagrams (and webs; see Section 2.2). However, there are contexts in which more generality is useful.

Definition 6 (Uniformly Proper sub-tableau)**.** Suppose T is a tableau with n rows and $S \subsetneq T$ is a (skew) sub-tableau. We call S *uniformly proper* if:

1. S has n rows

2. S is uniformly equivalent to a standard Young tableau

We call S a uniformly proper *rectangular* sub-tableau if in addition all of its rows have the same length. If T contains no uniformly proper rectangular sub-tableau, we say that T is *minimal.*

Given two skew tableaux T and T', we write TT' to refer to the tableau resulting from the horizontal concatenation of T and T' when such an operation makes sense. In particular, if T is an SYT that is not minimal, and thus has some uniformly proper rectangular sub-tableau S, we can write the tableau T as the horizontal concatenation $T = T_1ST_2$ where T_1 and T_2 are also sub-tableaux of T. Figure 2 gives an example.

Note that if we fix a uniformly proper rectangular sub-tableau S of T, there is a unique pair T_1, T_2 that decompose T as T_1ST_2. However, if T contains multiple uniformly proper rectangular sub-tableaux then there are many ways to decompose T as a horizontal concatenation.

$$\underset{T}{\begin{array}{|c|c|c|c|c|c|}\hline 1 & 2 & 6 & 7 & 14 & 19 \\ \hline 3 & 8 & 9 & 15 & 18 & 21 \\ \hline 4 & 10 & 11 & 16 & 20 & 23 \\ \hline 5 & 12 & 13 & 17 & 22 & 24 \\ \hline \end{array}} = \underset{T_1}{\begin{array}{|c|c|}\hline 1 & 2 \\ \hline 3 \\ \cline{1-1} 4 \\ \cline{1-1} 5 \\ \cline{1-1} \end{array}} \quad \underset{S}{\begin{array}{cccc} \cline{2-4} & \multicolumn{1}{|c|}{6} & \multicolumn{1}{c|}{7} & \multicolumn{1}{c|}{14} \\ \hline \multicolumn{1}{|c|}{8} & \multicolumn{1}{c|}{9} & \multicolumn{1}{c|}{15} & \\ \cline{1-3} \multicolumn{1}{|c|}{10} & \multicolumn{1}{c|}{11} & \multicolumn{1}{c|}{16} & \\ \cline{1-3} \multicolumn{1}{|c|}{12} & \multicolumn{1}{c|}{13} & \multicolumn{1}{c|}{17} & \\ \cline{1-3} \end{array}} \quad \underset{T_2}{\begin{array}{cc} \cline{2-2} & \multicolumn{1}{|c|}{19} \\ \hline \multicolumn{1}{|c|}{18} & \multicolumn{1}{c|}{21} \\ \hline \multicolumn{1}{|c|}{20} & \multicolumn{1}{c|}{23} \\ \hline \multicolumn{1}{|c|}{22} & \multicolumn{1}{c|}{24} \\ \hline \end{array}}$$

Figure 2: Decomposition of tableau T with uniformly proper rectangular sub-tableau S

We will see in Section 3 that the problem of determining the orbit length $|\mathcal{O}(T)|$ of any non-minimal tableau T can be reduced to determining the orbit lengths of a subset of its minimal uniformly proper sub-tableaux.

2.2 m-diagrams

We are motivated by open questions about webs, which are planar graphs that represent functions in a diagrammatic category for certain representations of quantum groups $U_q(\mathfrak{sl}_n)$ [8]. There is a rich literature on how promotion of tableaux corresponds to rotation of webs in the cases $n = 2$ and $n = 3$ [12, 17, 26]; but this is constrained for larger n by our limited understanding of webs in that case (though see [5] for a rotation-invariant basis when $n = 4$).

For this reason, we instead focus on an intermediary between webs and tableaux: m-diagrams, which are collections of arcs that satisfy certain noncrossing conditions.

Definition 7 (***m***-Diagram)**.** A *matching* $\mathcal{M}$ on the set $\{1, 2, \ldots, n\}$ is a set of pairs

$$\mathcal{M} = \{(i_1, j_1), (i_2, j_2), \ldots, (i_k, j_k)\} \subseteq \{1, 2, \ldots, n\} \times \{1, 2, \ldots, n\}$$

such that each element of $\{1, \ldots, n\}$ occurs in at most one pair. We often refer to the pair (i, j) as an *arc* and assume in our notation that $i \leqslant j$. We say that i, are the *endpoints* of the arc and that an integer i' is *on the arc* (i, j) if $i' \in \{i, j\}$ or *below the arc* (i, j) if $i < i' < j$.

A matching $\mathcal{M}$ is:

- *perfect* if every number $1, 2, \ldots, n$ is used on an arc;

- *crossing* if it contains two arcs $(i,j),(i',j') \in \mathcal{M}$ with $i < i' < j < j'$;
- *noncrossing* if it is not crossing;
- *with repetition* if it contains at least one arc of the form (i,i);
- *standard* if every integer i' below an arc (i,j) is itself on an arc.

An *m-diagram* on the set $\{1,2,\ldots,n\}$ is the union $\bigcup_{i=1}^{r} \mathcal{M}_i$ where each $\mathcal{M}_i$ is a noncrossing matching.

Note that an m-diagram may not itself be a noncrossing matching since arcs from one matching are allowed to cross arcs from another matching. An m-diagram may have arcs of the form (i,i) but is itself not a multiset, so each arc appears at most once in an m-diagram regardless of how many different matchings contain it.

We represent matchings and m-diagrams by drawing semicircular arcs in the upper half plane between the points i and j on the x-axis, as in Figure 3. The next lemma demonstrates a simple bijection between SYT and $m-$diagrams, the proof of which can be found in [17, Lemma 1] and [26, Prop. 2.4]. We include a sketch of the main arguments for completeness.

Lemma 8. *Let T be an SYT with r rows and content $\{1,\ldots,n\}$. For each $1 \leqslant i \leqslant r-1$ the following recursive process constructs a noncrossing matching $\mathcal{M}_i$ on the integers filling rows i and $i+1$ of T:*

1. *If row i of T has λ_i boxes then denote them by $t_i(1), t_i(2), \ldots, t_i(\lambda_i)$ and similarly for row $i+1$.*
2. *Create an arc $(t_i(j), t_{i+1}(1))$ where*
$$j = \max\{1 \leqslant s \leqslant \lambda_i : t_i(s) \leqslant t_{i+1}(1)\}.$$
3. *If $t_{i+1}(1),\ldots,t_{i+1}(\ell)$ are all on arcs then create an arc $(t_i(j), t_{i+1}(\ell+1))$ where*
$$j = \max\left\{\begin{array}{c} 1 \leqslant s \leqslant \lambda_i : t_i(s) \leqslant t_{i+1}(\ell+1) \text{ and} \\ (t_i(s), t_{i+1}(j')) \text{ is not an arc for any } j' \leqslant \ell \end{array}\right\}.$$

Proof. For each row $i+1$ and each entry $t_{i+1}(\ell)$ in that row, there are at least ℓ integers in row i of value at most $t_{i+1}(\ell)$ because the entries of T are increasing row- and column-wise. These integers are all distinct because the values in each row of T increase strictly and so the recursive process constructs an arc for each box in row $i+1$ of T.

Suppose $(t_i(\ell), t_{i+1}(\ell'))$ is an arc in the matching $\mathcal{M}_i$. If j is an integer on row $i+1$ with $j < t_{i+1}(\ell')$ then j is the endpoint of the arc created in an earlier step by the recursive construction to build $\mathcal{M}_i$. Thus $\mathcal{M}_i$ is a standard matching on the set of integers filling rows i and $i+1$ of T. Moreover the arc (j',j) satisfies $t_i(\ell) < j'$ since otherwise the recursive construction would have paired j with $t_i(\ell)$. Thus the arc (j',j) does not cross $(t_i(\ell), ti+1(\ell'))$. Similarly, if j is an integer on row i with $t_i(\ell) < j < t_{i+1}(\ell')$ then j must be on an arc $(j, t_{i+1}(\ell''))$ for some $\ell'' < \ell'$ else $j = t_i(\ell)$ by construction. So $\mathcal{M}_i$ is noncrossing. This completes the proof. $\square$

In the following result, all of the proofs are immediate from the previous lemma together with the definitions.

Corollary 9. *The algorithm in Lemma 8 defines a function $\varphi(T) = M_T$ from r-row SYT to m-diagrams built from $r-1$ matchings. In addition, all of the following hold:*

- *The number of arcs in matching $\mathcal{M}_i$ equals the number of boxes in row $i+1$ of T.*
- *Each matching $\mathcal{M}_i$ is without repetition.*
- *The matching $\mathcal{M}_i$ is standard with respect to the entries in rows i and $i+1$ of T.*
- *If T is a standard Young tableau on a rectangular Young diagram then $\varphi(T) = M_T$ is the union of $r-1$ matchings $\mathcal{M}_i$ of the same cardinality. Moreover every integer $1, 2, \ldots, |T|$ is one of three types: both the end of an arc in $\mathcal{M}_i$ and the start of an arc in $\mathcal{M}_{i+1}$, or the start of an arc on $\mathcal{M}_1$, or the end of an arc in $\mathcal{M}_{r-1}$.*

Figure 3 gives an example of an $m-$diagram corresponding to an SYT.

1	2	6	7	14	19
3	8	9	15	18	21
4	10	11	16	20	23
5	12	13	17	22	24

T

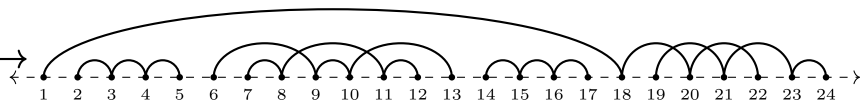

$\phi(T)$

Figure 3: Tableau T and its corresponding $m-$diagram $\phi(T)$

We define a rotation operation on m-diagrams algebraically as follows. Intuitively, it consists of connecting the endpoints of the boundary to form a circle, rotating the circle one step clockwise, and then disconnecting the circle to again form a boundary line.

Definition 10 (Rotation)**.** Denote by $\rho : \{1, 2, \ldots, n\} \to \{1, 2, \ldots, n\}$ the cyclic permutation given by $\rho(i) = i - 1 \mod n$. Then ρ induces a map from the set of matchings on $\{1, 2, \ldots, n\}$ to itself by sending each arc $(a, b) \mapsto (\rho(a), \rho(b))$. We call this map *rotation* and denote the image of a matching $\mathcal{M}$ under rotation by $\rho(\mathcal{M})$.

Figure 4 shows the rotation $\rho(\phi(T))$ of the $m-$diagram $\phi(T)$ from Figure 3.

The following two observations about rotation almost immediately follow from the definitions of matchings and rotations.

Lemma 11. *If $\mathcal{M}$ is a perfect matching then so is the rotation $\rho(\mathcal{M})$. If $\mathcal{M}$ is a non-crossing matching then so is the rotation $\rho(\mathcal{M})$.*

Proof. Rotation sends perfect matchings to perfect matchings because it permutes the endpoints of the arcs.

Suppose $\mathcal{M}$ is noncrossing. Every arc in $\mathcal{M}$ without endpoint 1, is simply shifted one unit to the left by ρ. Therefore, if two arcs cross in $\rho(\mathcal{M})$ one of them must be $\rho((1,k)) = (k-1,n)$. Say some arc $(i,j) \in \rho(\mathcal{M})$ crosses $(k-1,n)$. This implies $i < k-1 < j < n$ and also $1 < i+1 < k < j+1$. It follows that $\rho^{-1}((i,j)) = (i+1,j+1)$ and $(1,k)$ cross in $\mathcal{M}$. This contradiction proves the claim. $\square$

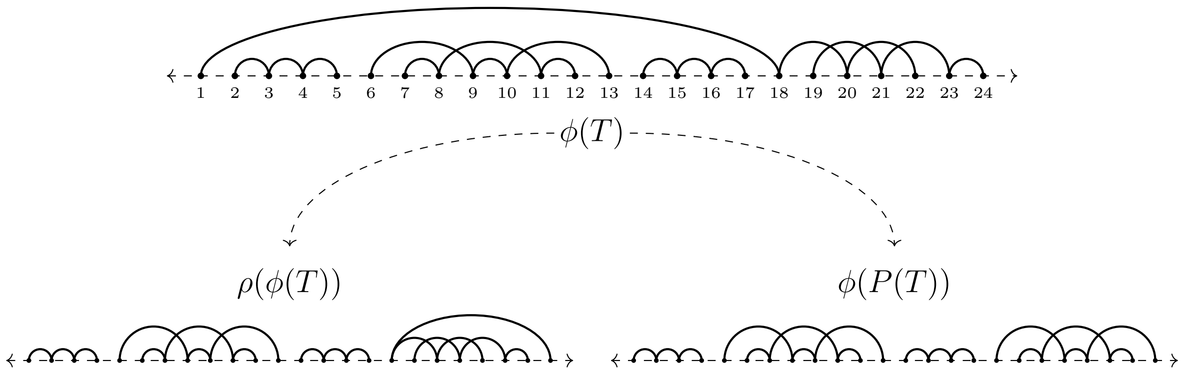

Figure 4: The rotation $\rho(\phi(T))$ compared to the $m-$diagram $\phi(P(T))$.

Just as rotation preserves the properties of being standard and noncrossing, we would like rotation to respect promotion, in the sense that rotating the m-diagram for an SYT T produces the m-diagram for the promotion $P(T)$. This does indeed hold for two-row rectangular SYT and for $\mathfrak{sl}_3$ webs coming from m-diagrams for three-row rectangular SYT [12, 26]. In general, however, promotion and rotation do not commute. For example, it is not true that the $m-$diagram $\phi(P(T))$ is equal to $\rho(\phi(T))$ for the tableau T in our running example, see Figure 4. Moreover, in general, $\rho(\varphi(T)) \neq \varphi(T')$ for any SYT T'. The next section describes a different way to connect rotation to promotion. The arguments in Section 3 utilize the idea of *sub-diagrams* and *components* of an $m-$diagram, which we introduce here.

Definition 12 (Sub-diagram and Component)**.** Consider an $m-$diagram $M = \{(a_i,b_i)\}_{i=1}^r$ where each (a_i,b_i) is an arc. Suppose $C \subsetneq M$ is a nonempty proper subcollection with $C = \{(a_{i_k},b_{i_k})\}_{k=1}^s$. We say C forms a *sub-diagram* of M if

- whenever a is an endpoint of some arc in C, all arcs in M with a as an endpoint are also in C and
- no arc in M but not C crosses any arc in C, namely no arc (a_j,b_j) with $j \notin \{i_1,\ldots,i_s\}$ crosses an arc in C.

The sub-diagram is *uniform* if its endpoints are all adjacent and a *component* if it has no proper subcollection that forms a sub-diagram. Two sub-diagrams C, C' are *equivalent* if $\rho^N(C) = C'$ for some N.

Example 13. We elucidate Definition 12 by illustrating the components of the $m-$diagram $\phi(T)$ from our running example, see Figure 5. The components of the

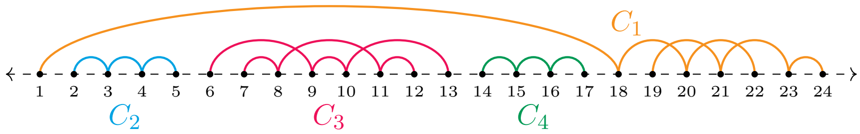

Figure 5: Components of $\phi(T)$

$m-$diagram $\phi(T)$ are C_1, C_2, C_3, and C_4. The components C_2, C_3, C_4 are uniform, whereas C_1 is non-uniform. Note that the components C_2 and C_4 are equivalent since $\rho^{12}(C_4) = C_2$. Any union of components forms a sub-diagram of $\phi(T)$. For example, $C_2 \cup C_3$ forms a uniform sub-diagram, whereas both $C_1 \cup C_3$ and $C_2 \cup C_4$ form non-uniform sub-diagrams.

3 Determining Orbit Lengths

Our main result is an identification between the orbit lengths of rectangular SYT and the rotational symmetry of their corresponding $m-$diagrams. This identification allows us to explicitly compute the orbit length of a non-minimal tableau by only considering certain sub-tableaux. To this end, we provide a simple algorithm to compute orbit lengths of non-minimal SYT.

Throughout this section we fix a non-minimal *rectangular* SYT $\boldsymbol{T}$ with uniformly proper rectangular sub-tableau $\boldsymbol{S}$. It will often be convenient to consider T as the horizontal concatenation T_1ST_2 where the sub-tableau T_1 is non-empty, i.e. $|T_1| \geqslant 1$. As an example, recall the tableau T from Figure 2, with its uniformly proper rectangular sub-tableau S.

We begin by building a correspondence between uniformly proper rectangular sub-tableaux of T and uniform sub-diagrams of its corresponding $m-$diagram $\phi(T)$. First, we show that the arcs generated by the algorithm in Lemma 8 either have both end points in S or neither end point in S.

Lemma 14. *Suppose S is a uniformly proper rectangular sub-tableau of T. If the $m-$diagram $\varphi(T)$ contains an arc (a, b) with either a an entry of S or b an entry of S, then both a and b are entries of S.*

Proof. Write T as the horizontal concatenation $T = T_1ST_2$ and suppose that $a = T_{ij}$. Then, since (a, b) is an arc in $\varphi(T)$, we must have that b is on row $i+1$ of T.

First, suppose that b is an entry of S. Since every entry of T_2 is greater than every entry of T_1S, we must have that a is an entry of T_1S. Note that since T_1 is a proper sub-tableau of T, the length of row i of T_1 is at least the length of row $i+1$ of T_1. Thus, when the algorithm in Lemma 8 is creating arcs that begin with entries in row $i+1$ of T, every entry on row $i+1$ of T_1 will be matched to an entry on row i of T_1. Since we also have that S is rectangular, for each entry on row $i+1$ of S, there is at least one entry on row i of S that is yet to be matched by the algorithm in Lemma 8. Moreover, since S is uniformly equivalent to an SYT, for each entry on row $i+1$ of S, there is at least one entry on row i of S that has lower value. As each entry of S is greater than every entry of T_1, it follows that each entry on row $i+1$ of S is matched to an entry on row i of S. Thus, a is an entry of S.

Now, suppose a is an entry of S. Since each entry of T_1 is less than every entry of S, we must have that b is an entry of ST_2. By the above argument, every entry on row $i+1$ of S is matched to some entry on row i of S. Since S is rectangular, the number of arcs beginning at an entry on row $i+1$ of S is equal to the number of arcs ending at an entry on row i of S. It follows that b is an entry on row $i+1$ of S. $\square$

We can now identify uniformly proper rectangular sub-tableaux of T with uniform sub-diagrams of the $m-$diagram $\phi(T)$. Moreover, by applying this correspondence recursively, we see that minimal uniformly proper sub-tableaux are in correspondence with uniform components of $\phi(T)$.

Lemma 15. *Let $M = \varphi(T)$. We have the following correspondences:*

1. *The set of uniformly proper rectangular sub-tableaux of T is in bijection with the uniform sub-diagrams of M.*

2. *The set of minimal uniformly proper rectangular sub-tableaux of T is in bijection with the uniform components of M.*

Proof. Note that (2) is a simple consequence of (1) and so we only prove (1).

Fix a uniformly proper rectangular sub-tableau S of T and let C_S be the collection of arcs in M with an endpoint that is an entry of S. By Lemma 14, any arc in C_S must have both endpoints in S. Note that this means that no arc of M with an endpoint outside of S can cross an arc in C_S. Thus, we have that C_S is a sub-diagram of M. As S is a *uniformly* proper sub-tableau of T, it follows that the endpoints of C_S are all adjacent and so C_S is a uniform sub-diagram of M.

Now, fix a uniform sub-diagram C of M. Suppose that the endpoints of arcs in C are $\{k, k+1, \ldots, k+\ell\}$ and consider the sub-tableau S of T with entries $\{k, k+1, \ldots, k+\ell\}$. We show that S is a uniformly proper rectangular sub-tableau. All parts of this proof amount to showing that violating any part of the definition of a uniformly proper rectangular sub-tableau is equivalent to having an arc in M with one endpoint an entry in S and the other endpoint not an entry in S.

First, note that the sub-diagram C is a union of components of M. In each component, there are exactly two vertices that have degree 1 (in the graph theory sense), while all other vertices have degree 2. By Corollary 9, these degree one vertices are entries in either the first or last row of T. By construction, exactly one of these vertices is in the first row and the other is in the last row. It follows that S has the same number of rows as T. Moreover, both the first and last row of S have the same number of boxes and thus S is a rectangular sub-tableau of T.

Suppose that when S is left-justified, it is not standard. Since S is a sub-tableau of T, the rows of S are increasing and thus if S is not standard when left-justified, there must be some column that is not increasing. Choose j to be the smallest value such that the j^{th} column of S is not increasing. Then for some row i we have that $S_{ij} < S_{(i-1)j}$ and for all $j' < j$, the columns of S are increasing. As entries to the left of S_{ij} are of lower value and are in increasing columns, the algorithm in Lemma 8 matches each entry $S_{ij'}$ for $j' < j$ to some entry on row $i-1$ of S. However, we then have that the algorithm cannot match $S_{(i+1)j}$ to any entry on row i of S. Thus, the arc starting at S_{ij} in M has an endpoint that is not an entry of S. This contradicts the definition of S.

This proves that S must be a uniformly proper rectangular sub-tableau and therefore the map between these sub-tableaux and uniform sub-diagrams is a bijection. □

Given the correspondence between the internal structure of T and the geometric structure of $\phi(T)$, we now consider how the promotion operation on T affects these structures. The following result shows that the uniformly proper sub-tableaux of T are preserved under the action of promotion T. Our key insight here is that the "sliding path" of the empty box during promotion can only move horizontally through a uniformly proper rectangular sub-tableau, as in the schematic of Figure 6.

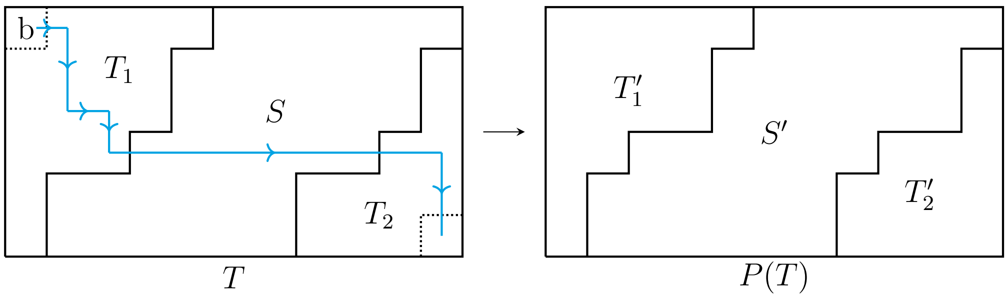

Figure 6: Sliding path of b through T and structure of $P(T)$

Lemma 16. *Let T be an SYT with uniformly proper rectangular sub-tableau S so that $T = T_1ST_2$ with $|T_1| \geqslant 1$. Then, $P(T) = T_1'S'T_2'$ where $T_1'T_2' \equiv P(T_1T_2)$ and S' is a uniformly proper rectangular sub-tableau of $P(T)$ that is uniformly equivalent to S.*

Proof. Consider the sliding path of the empty box b during the promotion of T.

Each element of T_1 is less than every element of S so b can only slide into S when its neighbours to the right and below are both in S or outside of the tableau. Thus, b can only slide into S when it reaches the bottom row of a rectangular sub-shape of T_1. If b reaches the bottom row of T_1 then b can only slide horizontally in S. If b does not reach the bottom row of T_1 then consider its two neighbours in S as shown in Figure 7. Since S is uniformly proper, the entry in the box below b is greater than the entry in the box to the right of b and thus b slides to the right. The same argument shows that b only slides horizontally until it is either at the end of the row or at least one of its neighbours is in T_2. Suppose b has one neighbour in S and one neighbour in T_2. Each row of S is the same length so the box below b is in T_2. All entries in T_2 are larger than the entries in S so b continues to slide horizontally. Thus b slides horizontally until both of its neighbours are in T_2 or until it is at the end of the row, see Figure 6 for a schematic.

We have proven that b only slides horizontally in S. This means that the only way promotion changes S is by sliding one row to the left by one box and decreasing entries by 1. Call the resulting tableau S'. Then S' is equivalent to S by construction. Moreover, they are uniformly equivalent because 1 is subtracted from each entry of S to form S'.

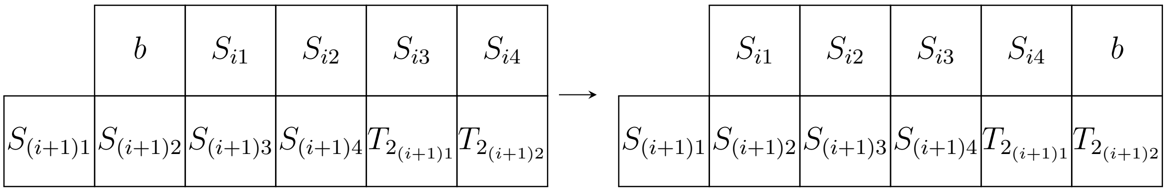

Figure 7: Comparing entries as b slides through S

We have shown S' is a uniformly proper rectangular sub-tableau of $P(T)$ and so we can write $P(T)$ as the horizontal concatenation $P(T) = T_1'S'T_2'$. We now show $T_1'T_2' \equiv P(T_1T_2)$ by again considering the sliding path of b. Let P_1 denote the part of the sliding path of b that is in T_1, P_2 the part of the path in S, and P_3 the part of the path in T_2.

Consider the tableau T_1T_2 and the sliding path of the empty box b during its promotion. Since each element of T_1 is smaller than every element of T_2 the empty box b slides into T_2 when its neighbours to the right and below are in T_2 or outside of the tableau entirely. Promotion is defined from pairwise comparisons so the sliding path of b in T_1 is exactly P_1. After sliding along P_1 the empty box b has neighbors c_1, c_2, to the right and below b respectively, that are either in T_2 or outside of the tableau. Since b only slides horizontally in S we know that after sliding along the path P_2 in T, the same entries c_1, c_2 neighbour b. Thus, the remainder of sliding path of b in T_1T_2 is P_3 and so the whole sliding path is P_1P_3. It follows that $T_1'T_2' \equiv P(T_1T_2)$ as desired. $\square$

Thus, we have that the uniformly proper rectangular sub-tableaux of T that do not contain 1 are preserved during promotion, though their entries are all decremented by 1. A simple consequence of this result along with the correspondence in Lemma 15 is that uniform sub-diagrams of the $m-$diagram $\phi(T)$ that do not contain arcs ending at 1 are also in some sense preserved during promotion: for each uniform component C of $\phi(T)$ that does not have 1 as an endpoint, $\rho(C)$ is a uniform sub-diagram of $\phi(P(T))$.

Corollary 17. *If C is a uniform sub-diagram of $\varphi(T)$ that does not contain the vertex 1, $\varphi(P(T))$ contains the uniform sub-diagram $\rho(C)$, where ρ is the rotation operation defined in Section 2.2.*

Proof. By the correspondence given in Lemma 15, the uniform sub-diagram C corresponds to a uniformly proper sub-tableau T_C of T. As C does not contain an arc that ends at 1, we have that 1 is not an entry of T_C. Thus, T can be written as $T = T_1T_CT_2$ with $|T_1| \neq 0$. By Lemma 16, $P(T)$ contains the sub-tableau T_C' whose entries are the same as T_C with one subtracted from each entry. Again by the correspondence in Lemma 15, T'_C corresponds to a uniform sub-diagram C' of $\varphi(P(T))$. As T_C and T'_C are uniformly equivalent it is clear from the algorithm given in Section 2.2 that entries of T'_C will be matched in the same order as the entries of T_C and thus the arcs in C' will simply be the left translation of the arcs of C. It follows that $C' = \rho(C)$, concluding the proof. $\square$

Our previous results show that the only component of the $m-$diagram $\phi(T)$ that is *not* preserved during promotion is the component C that has an arc ending at 1. We wish to describe how the structure of $\phi(T)$ evolves as the promotion operator is applied to T. Motivated by this, we examine how promotion alters substructures of T that correspond to the components of $\phi(T)$.

Note that for each component C of $\phi(T)$ we can construct a rectangular tableau T_C whose content we denote ∂C and whose $m-$diagram is C itself. In fact, T_C comes from left justifying the collection of boxes in T with entries ∂C. As an example, we show the tableaux corresponding to each component in our running example in Figure 8. The tableau T_C is necessarily a collection of boxes inside T so we now characterize how the structure of T_C within T changes as we apply the promotion operator.

Definition 18 (Component Promotion)**.** Let C be a component of $\phi(T)$ and construct the corresponding tableau T_C. With a slight abuse of language and notation, we define the promotion $P(T_C)$ of T_C as follows:

1. If $1 \notin \partial C$, form $P(T_C)$ by decrementing each entry of T_C by 1.
2. If $1 \in \partial C$, form $P(T_C)$ by
   (a) removing 1 from the top left corner of T_C,
   (b) performing the sequence of sliding moves outlined in Definition 2,
   (c) decrementing each entry of T_C by 1,
   (d) filling the empty box with $|T|$.

We illustrate the component promotions of components in our running example in Figure 8. Our next result shows that for any component C of the $m-$diagram $\phi(T)$, the collection of boxes in $P(T)$ with entries $\rho(\partial C)$ gives the tableau $P(T_C)$.

Lemma 19. *For each component C of $\phi(T)$, left-justifying the collection of boxes with content $\rho(\partial C)$ in $P(T)$ produces the tableau $P(T_C)$.*

Proof. Let S be the sub-tableau of T consisting of all boxes of T with entries j such that $\min\{i \in \partial C\} \leqslant j \leqslant \max\{i \in \partial C\}$. Note that S is the minimal uniformly proper rectangular sub-tableau of T that contains each element of ∂C, or is equal to T if ∂C contains both 1 and n. The collection of boxes in S with content ∂C form the tableau T_C once left justified.

First, suppose $1 \notin \partial C$ and so $1 \notin S$. By Lemma 16, subtracting 1 from each entry of S yields a uniformly proper rectangular sub-tableau of $P(T)$. In particular, the boxes with content $\rho(\partial C)$ within $P(T)$ form the tableau $P(T_C)$ as defined in Definition 18.

Now, suppose $1 \in \partial C$. Then, we can write T as the horizontal concatenation $T = SR$ where R is the uniformly proper rectangular sub-tableau of T with all entries greater than the maximum element of ∂C. By Lemma 16, the promotion $P(T)$ can be written as the horizontal concatenation $P(T) = S_1 R' S_2$ where R' is the sub-tableau of $P(T)$ formed by subtracting 1 from each entry of R and S_2 consists of only the box containing n. Moreover, we have the equivalence $S_1 S_2 \equiv P(S)$. Note that replacing the maximum entry of $P(S)$ with the maximum entry n of T yields $S_1 S_2$.

If C is a uniform component of $\phi(T)$, then $S = T_C$ and so $S_1 S_2 = P(T_C)$ as defined in Definition 18. If C is not a uniform component of $\phi(T)$ then the boxes in S whose entries are not in ∂C form U, a uniformly proper rectangular sub-tableau of T. Let T_{C_1} be the collection of boxes in S to the left of U and T_{C_2} the boxes of S to the right of U so the S is the horizontal concatenation $S = T_{C_1} U T_{C_2}$. Then, by Lemma 16, $P(S) = T'_{C_1} U' T'_{C_2}$ where U' is formed by subtracting 1 from each entry of U and $T_{C'} T'_{C_2} \equiv P(T_C)$. Replacing the maximum entry of T'_{C_2} with the maximum entry n of T yields $P(T_C)$, completing the proof. $\square$

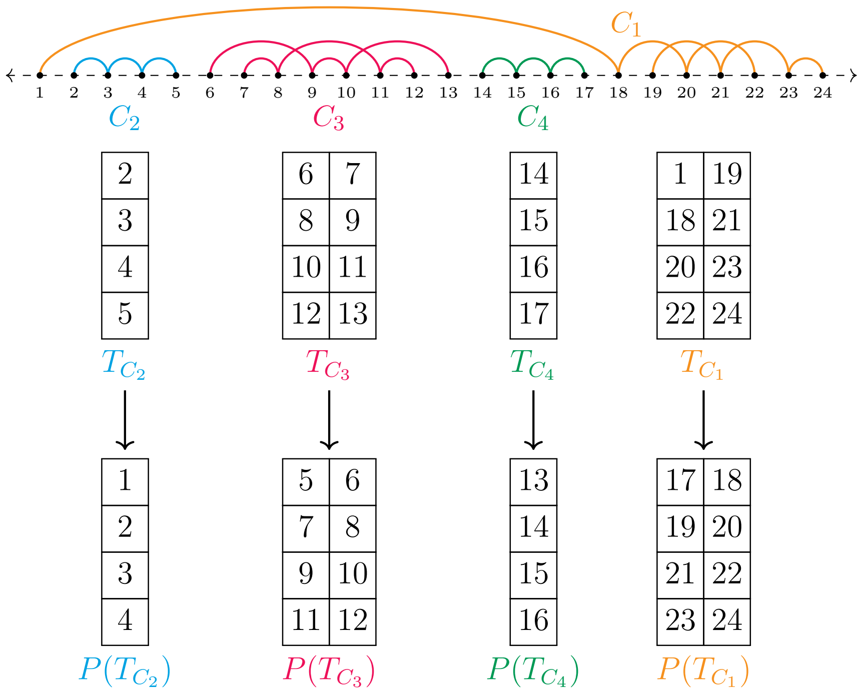

Figure 8: The components of the $m-$diagram $\phi(T)$ along with their corresponding tableau T_{C_i} and component promotions $P(T_{C_i})$.

Remark 20. An equivalent definition of component promotion when $1 \in \partial C$ can be formulated by constructing a specific SYT to represent the component C. Suppose C has the first ℓ vertices of $\phi(T)$ as endpoints, so $\partial C = \{t_1 < t_2 < \ldots < \ldots < t_m\}$ with $t_1 = 1, \ldots, t_\ell = \ell$. For each $k \leqslant \ell$, we may determine the $k-$fold component promotion of T_C as follows:

1. Form the SYT T'_C by replacing entry t_i with i.

2. Compute the $k-$fold promotion $P^k(T'_C)$ using the algorithm in Definition 2.

3. Replace the content of $P^k(T'_C)$ with the set $\rho^k(\partial C)$ in order from smallest to largest.

The results of Lemma 19 have a natural geometric interpretation. As in Corollary 17, we see that the only component of $\phi(T)$ whose structure is not preserved in promotion is the component C_1 with $1 \in \partial C_1$. If C is any other component of $\phi(T)$, we see that $\rho(C)$ is a component of $\phi(P(T))$. For instance, consider our running example in Figure 4. All three components nested under the arc $(1, 18)$ in $\phi(T)$ look exactly the same in $\rho(\phi(T))$ after rotation; however, the component containing arc $(1, 18)$ in $\phi(T)$ looks different both from the rightmost component in $\rho(\phi(T))$ and from the rightmost component of $\phi(P(T))$. Two conclusions follow:

1. Not every component C of $\phi(T)$ gives rise to a component $\rho(C)$ of $\phi(P(T))$.

2. Nonetheless, if C is the component of $\phi(T)$ containing boundary point 1, there is a component of $\phi(P(T))$ with exactly the same endpoints as $\rho(C)$. Moreover, this component is $\phi(P(T_C))$ with $P(T_C)$ as defined in Definition 18.

The next corollary records these observations.

Corollary 21. *Choose a sub-diagram C of $\phi(T)$. Suppose that $\partial C = \{a_{i_k}, b_{i_k}\}_{k=1}^{s}$ is the set of endpoints of C and T_C is the tableau corresponding to C.*

1. *The arcs with endpoints $\rho(\partial C)$ in $\varphi(P(T))$ form a sub-diagram of $\varphi(P(T))$.*

2. *If C is a component, the collection of arcs with endpoints $\rho(\partial C)$ in $\phi(P(T))$ form the component $\phi(P(T_C))$.*

Proof. This is a simple application of Lemma 19. □

From Corollary 21, we see that the partition of the boundary of $\phi(P(T))$ induced by its components is given by a left-translation of the partition of the boundary of $\phi(T)$. It follows that performing $|\mathcal{O}(T)|$ left-translations maps the boundary of $\phi(T)$ to itself. We make this precise using a notion of *rotational symmetry.*

Definition 22 (Rotational Symmetry)**.** Let $C_1, \ldots, C_k$ be the components of the $m-$diagram $\phi(T)$ and ∂C_i the set of endpoints of component C_i. Then $\phi(T)$ has order N rotational symmetry if N is the smallest positive integer such that the following equality holds:

$$\{\rho^N(\partial C_1), \ldots, \rho^N(\partial C_k)\} = \{\partial C_1, \ldots, \partial C_k\}.$$

We now show that the orbit length $|\mathcal{O}(T)|$ is a multiple of the rotational symmetry of its $m-$diagram.

Lemma 23. *Suppose $\phi(T)$ has order N rotational symmetry. Then N divides the orbit length $|\mathcal{O}(T)|$.*

Proof. First, let $C_1, \ldots, C_k$ be the components of $\phi(T)$ and $C_1', \ldots, C_\ell'$ the components of $\phi(P(T))$. For any component C, let ∂C be the set of endpoints of C. Then by construction, we see that $\sqcup_{i=1}^k \partial C_i$ and $\sqcup_{i=1}^\ell \partial C_i'$ are both partitions of the set $[n] = \{1, \ldots, n\}$. Furthermore, by Corollary 21, we have that $\bigsqcup_{i=1}^k \rho(\partial C_i) = \bigsqcup_{i=1}^\ell \partial C_i'$. In other words, the set partition coming from $\phi(P(T))$ is a one-unit leftward shift modulo n of the set partition coming from $\varphi(T)$. In particular, $k = \ell$.

Since $\varphi(P^{|\mathcal{O}(T)|}(T)) = \varphi(T)$, it follows that $\bigsqcup_{i=1}^k \rho^{|\mathcal{O}(T)|}(\partial C_i) = \bigsqcup_{i=1}^k \partial C_i$. Since $\phi(T)$ has order N rotational symmetry, we know N is the smallest positive leftward shift modulo n that maps the set partition coming from $\phi(T)$ onto itself. Now $|\mathcal{O}(T)| = Nq + r$ for some $q, r \in \mathbb{Z}$ with $0 \leqslant r < N$, and this means $\bigsqcup_{i=1}^k \rho^r(\partial C_i) = \bigsqcup_{i=1}^k \partial C_i$. Since N is minimal, we must have that $r = 0$ and so N divides $|\mathcal{O}(T)|$. $\square$

Remark 24. For a rectangular tableau T, we have seen that the components of the $m-$diagram $\varphi(T)$ induce a specific set partition $\Lambda_T = \sqcup_{C \in \varphi(T)} \partial C$ of the set $[|T|]$. Now, let Λ be some partition of the set $[nm]$ for some $n, m \in \mathbb{N}$, and consider the set

$$\mathcal{T}_\Lambda = \left\{T \in SYT(n \times m) : \Lambda_T \in \{\Lambda, \rho(\Lambda), \rho^2(\Lambda), \rho^3(\Lambda), \rho^4(\Lambda), \rho^5(\Lambda), \ldots\}\right\}$$

where we interpret $\rho^N(\Lambda)$ to mean applying the map ρ to each subset in Λ. In other words, $\mathcal{T}_\Lambda$ is the set of all tableaux that induce partitions which are rotationally equivalent to Λ.

Then, for each $T \in \mathcal{T}_\Lambda$, we have that $\mathcal{O}(T) \subseteq \mathcal{T}_\Lambda$ from Corollary 21. In this way, we get a lower bound $|\{\text{nonempty } \mathcal{T}_\Lambda : \Lambda \text{ is a partition of } [nm]\}|$ on the number of promotion orbits in $SYT(n \times m)$ and an upper bound $|\mathcal{T}_{\Lambda_T}|$ on $|\mathcal{O}(T)|$.

We now provide an algorithm for determining the orbit lengths of non-minimal tableaux. To do so, we introduce an integer ℓ that counts rotations until *both* the boundaries of each component match (via rotational symmetry) *and* the arcs above "look the same."

Theorem 25. *The orbit length $|\mathcal{O}(T)|$ can be determined as follows:*

1. *Let N be the order of rotational symmetry of $\phi(T)$.*
2. *Define ℓ as*

$$\ell = \min\{k \geqslant 1 : \rho^{kN}(\partial C_i) = \partial C_j \implies P^{kN}(T_{C_i}) = T_{C_j} \forall i\}$$

where T_{C_i} is the tableau corresponding to C_i.

Then, the equality $|\mathcal{O}(T)| = \ell N$ holds.

Proof. By Lemma 23 we have that if $\phi(T)$ has order N rotational symmetry, then $N \big| |\mathcal{O}(T)|$. We complete the proof by showing that ℓ as defined in step (2) is the smallest positive integer such that $|\mathcal{O}(T)| \big| \ell N$.

Note that for each component C_i of $\phi(T)$ we have that $\rho^{\ell N}(\partial C_i) = \partial C_j$ for some j by the definition of N. Iterated applications Corollary 21 yields that the component of $\phi(P^{\ell N}(T))$ with endpoints equal to ∂C_j is the component $\phi(P^{\ell N}(T_{C_i}))$. Define C_j' to be the component of $\phi(P^{\ell N}(T))$ with endpoints equal to ∂C_j. Since ℓ is chosen so that whenever $\rho^{\ell N}(\partial C_i) = \partial C_j$ we have that $P^{\ell N}(T_{C_i}) = T_{C_j}$, we see that the algorithm in Lemma 8 constructs the arcs in C'_j in the same order that it constructs the arcs in C_j. It follows that $C'_j = C_j$ and so we have that $\phi(P^{\ell N}(T)) = \phi(T)$. It follows that $|\mathcal{O}(T)|\big|\ell N$.

Now, if $k < \ell$, there is some component C_i of $\phi(T)$ such that $\rho^{kN}(\partial C_i) = \partial C_j$ and $P^{kN}(T_{C_i}) \neq T_{C_j}$. It follows that the component of $P^{kN}(T)$ with endpoints equal to ∂C_j is not equal to C_j and so $|\mathcal{O}(T)|$does not divide kN. This completes the proof. $\square$

Example 26. As an example, both of the $m-$diagrams shown below have the same order of rotational symmetry because both have two components, each with 8 boundary points.

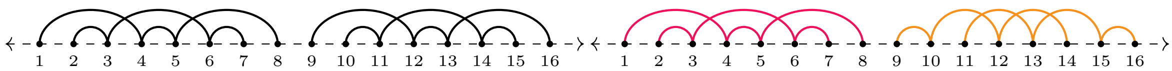

Thus $N = 8$ in the notation of the previous Theorem. The $m-$diagram on the left has $\ell = 1$ while the $m-$diagram on the right has $\ell = 2$. Intuitively, this is because the two components in the $m-$diagram on the left "look the same" but "look different" in the $m-$diagram on the right. Formally, we need to compute promotions of the tableaux corresponding to the four components. Three of the components above have corresponding tableau that is uniformly equivalent to T_C below, while the fourth is $T_{C'}$ below.

$$T_C = \begin{array}{|c|c|}\hline 1 & 2 \\ \hline 3 & 4 \\ \hline 5 & 6 \\ \hline 7 & 8 \\ \hline \end{array} \qquad T_{C'} = \begin{array}{|c|c|}\hline 9 & 11 \\ \hline 10 & 13 \\ \hline 12 & 15 \\ \hline 14 & 16 \\ \hline \end{array}$$

As a 4×2 tableau, note that T_C has promotion order 2 so $\ell = 1$ for the $m-$diagram on the left. Also $P(T_C)$ is uniformly equivalent to $T_{C'}$. So $P^8(T_{C'}) \neq T_C$ and $\ell = 2$ for the $m-$diagram on the right, as claimed.

Remark 27. While Theorem 25 gives us a method to compute the orbit length of any non-minimal tableau, for many examples there may be shortcuts. For example, if the $m-$diagram $\phi(T)$ has order $|T|$ rotational symmetry, it is clear that $|\mathcal{O}(T)| = |T|$. As well, by the results of [6], the orbit length $|\mathcal{O}(T)|$ must divide $|T|$. It follows that N must divide $|T|$, reducing the set of possible orders of rotational symmetry to check. Moreover, once N has been found, in step (4) of Theorem 25 we need only check values of ℓ such that $\ell N\big||T|$.

Following the algorithm in Theorem 25, we see that the orbit length $|\mathcal{O}(T)|$ is determined by examining orbits of a set of minimal tableaux. While there is no known method for identifying the orbit lengths of minimal tableaux, these tableaux are typically much smaller than T and thus directly computing their orbit lengths is much less computationally expensive than computing the entire promotion orbit of T.

Example 28. We can now calculate the promotion orbit length of our running example T. The $m-$diagram $\phi(T)$ has four components, C_1, C_2, C_3, C_4.

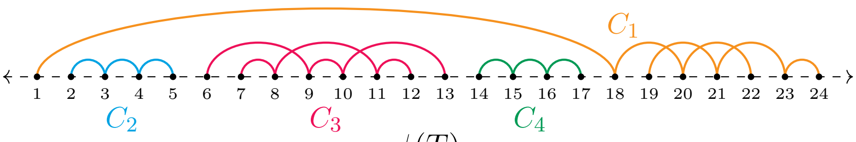

$\phi(T)$

The sets of endpoints for each component are the following:

$$\begin{aligned}
\partial C_1 &= \{1, 18, 19, 20, 21, 22, 23, 24\}\\
\partial C_2 &= \{2, 3, 4, 5\}\\
\partial C_3 &= \{6, 7, 8, 9, 10, 11, 12, 13\}\\
\partial C_4 &= \{14, 15, 16, 17\}.
\end{aligned}$$

Note that the following equalities hold:

$$\rho^{12}(\partial C_1) = \partial C_3 \quad \rho^{12}(\partial C_2) = \partial C_4 \quad \rho^{12}(\partial C_3) = \partial C_1 \quad \rho^{12}(\partial C_4) = \partial C_2.$$

This is the minimal value of N such that $\sqcup_{i=1}^4 \rho^N(\partial C_i) = \sqcup_{i=1}^4 \partial C_i$ and so $\phi(T)$ has order 12 rotational symmetry. As the orbit length $|\mathcal{O}(T)|$ must divide 24, either $|\mathcal{O}(T)| = 12$ or $|\mathcal{O}(T)| = 24$. We now need to calculate the 12-fold promotions of each tableau T_{C_i} corresponding to the components C_i.

$$\underset{T_{C_1}}{\begin{array}{|c|c|}\hline 1 & 19\\\hline 18 & 21\\\hline 20 & 23\\\hline 22 & 24\\\hline\end{array}} \qquad \underset{T_{C_2}}{\begin{array}{|c|}\hline 2\\\hline 3\\\hline 4\\\hline 5\\\hline\end{array}} \qquad \underset{T_{C_3}}{\begin{array}{|c|c|}\hline 6 & 7\\\hline 8 & 9\\\hline 10 & 11\\\hline 12 & 13\\\hline\end{array}} \qquad \underset{T_{C_4}}{\begin{array}{|c|}\hline 14\\\hline 15\\\hline 16\\\hline 17\\\hline\end{array}}$$

Recall that whenever $1 \notin \partial C_i$, the promotion $P(T_{C_i})$ is achieved by simply decrementing each entry of T_{C_i} by 1, which corresponds to simply translating the component C_i once to the left in $\phi(T)$. So, we have that $P^{12}(T_{C_4}) = T_{C_2}$. We now consider the promotions of $T_{C_1}, T_{C_2}, T_{C_3}$. As each of these components has an endpoint within the first 12 vertices of $\phi(T)$, the structure of each component will change as the promotion operator is applied to T. First, we see that the 12-fold promotion of T_{C_1} is given by

$$\underset{T_{C_1}}{\begin{array}{|c|c|}\hline 1 & 19\\\hline 18 & 21\\\hline 20 & 23\\\hline 22 & 24\\\hline\end{array}} \longrightarrow \underset{P(T_{C_1})}{\begin{array}{|c|c|}\hline 17 & 18\\\hline 19 & 20\\\hline 21 & 22\\\hline 23 & 24\\\hline\end{array}} \cdots\cdots\rightarrow \underset{P^{12}(T_{C_1})}{\begin{array}{|c|c|}\hline 6 & 7\\\hline 8 & 9\\\hline 10 & 11\\\hline 12 & 13\\\hline\end{array}}$$

and so $\rho^{12}(\partial C_1) = \partial C_3$ and $P^{12}(T_{C_1}) = T_{C_3}$. The 12-fold promotion of T_{C_2} is found as follows:

$$\underset{T_{C_2}}{\begin{array}{|c|}\hline 2 \\ \hline 3 \\ \hline 4 \\ \hline 5 \\ \hline \end{array}} \longrightarrow \underset{P(T_{C_2})}{\begin{array}{|c|}\hline 1 \\ \hline 2 \\ \hline 3 \\ \hline 4 \\ \hline \end{array}} \dashrightarrow \underset{P^5(T_{C_2})}{\begin{array}{|c|}\hline 21 \\ \hline 22 \\ \hline 23 \\ \hline 24 \\ \hline \end{array}} \dashrightarrow \underset{P^{12}(T_{C_2})}{\begin{array}{|c|}\hline 14 \\ \hline 15 \\ \hline 16 \\ \hline 17 \\ \hline \end{array}}$$

So we have that $\rho^{12}(\partial C_2) = \partial C_4$ and $P^{12}(T_{C_2}) = T_{C_4}$. Note that we calculate $P^5(T_{C_2})$ from $P(T_{C_2})$ using the arguments in Remark 20. Finally, the 12-fold promotion of T_{C_3} is

$$\underset{T_{C_3}}{\begin{array}{|c|c|}\hline 6 & 7 \\ \hline 8 & 9 \\ \hline 10 & 11 \\ \hline 12 & 13 \\ \hline \end{array}} \dashrightarrow \underset{P^5(T_{C_3})}{\begin{array}{|c|c|}\hline 1 & 2 \\ \hline 3 & 4 \\ \hline 5 & 6 \\ \hline 7 & 8 \\ \hline \end{array}} \dashrightarrow \underset{P^{12}(T_{C_3})}{\begin{array}{|c|c|}\hline 1 & 19 \\ \hline 18 & 21 \\ \hline 20 & 23 \\ \hline 22 & 24 \\ \hline \end{array}}$$

and so $\rho^{12}(\partial C_3) = \partial C_1$ and $P^{12}(T_{C_3}) = T_{C_1}$. Thus, the orbit length $|\mathcal{O}(T)|$ is 12.

4 Application: Promotion of Rectangular Semi-Standard Tableaux

We now extend the results of Section 3 to the case of semi-standard Young tableaux.

We begin with an overview of (column) semi-standard Young tableaux, paying particular attention to the promotion operator. A *(column) semi-standard Young tableau (SSYT)* is a filling of the Young diagram for λ with the numbers $1, 2, \ldots, n$ so that each number appears at least once, rows strictly increase left-to-right, and columns weakly increase top-to-bottom. If each number i appears e_i times in T then we denote the content $\{1^{e_1}, 2^{e_2}, \ldots, n^{e_n}\}$. Generically, the content of an SSYT is a multiset.

Remark 29. Usually *semi-standard* refers to tableaux in which columns strictly increase and rows are weakly increasing. It is for this reason that we emphasize *column* in our terminology. Note that each column semi-standard tableau is the transpose of a (row) semi-standard tableau.

Given an SSYT of shape λ, there is a natural map ψ that constructs an SYT of the same shape. Suppose T has content $\{1^{e_1}, \ldots, n^{e_n}\}$. The SYT $\psi(T)$ is constructed via the following procedure.

1. Relabel each 1 in T sequentially from top to bottom using the set $\{1, 2, \ldots, e_1\}$.

2. For each $i > 1$, relabel each entry i sequentially from top to bottom using the set $\{(e_1 + \ldots + e_{i-1}) + 1, (e_1 + \ldots + e_{i-1}) + 2, \ldots, (e_1 + \ldots + e_{i-1}) + e_i\}$.

Note that the map ψ is the usual standardization on SSYT transposed. We give an example of an SYT constructed with ψ in Figure 9. Later, we will see that the map ψ commutes with the promotion operator in a natural way. First, we prove that $\psi(T)$ is indeed an SYT of the same shape as T.

1	2	3	6	9	12
3	4	5	6	9	12
3	6	7	8	9	12
3	6	9	10	11	12

T

$\longrightarrow$

1	2	3	9	15	21
4	7	8	10	16	22
5	11	13	14	17	23
6	12	18	19	20	24

$\psi(T)$

Figure 9: The column SSYT T and its corresponding SYT $\psi(T)$

Lemma 30. *Suppose T is a column SSYT with content $\{1^{e_1}, 2^{e_2}, \ldots, n^{e_n}\}$. Then $\psi(T)$ is an SYT of the same shape with content $\{1, 2, \ldots, (e_1 + \ldots + e_n)\}$.*

Proof. As the map ψ simply relabels the entries of T, it is clear that T and $\psi(T)$ are the same shape.

Since the entries of T strictly increase left-to-right, no number can be repeated twice in the same row. Thus, all copies of each number i in T appear in a skew strip of width at most one. This means the sequential renumbering for each i is unambiguous. If two copies of i appear in the same column of T then the corresponding boxes in $\psi(T)$ increase strictly from top to bottom. For all other $i < j$ in T, the numbers in the corresponding boxes of $\psi(T)$ are still increasing by construction. So $\psi(T)$ is both row-strict and column-strict and is thus an SYT. $\square$

A simple consequence of the definition of ψ is that it is injective on the set of all SSYT with the same shape and content. That is, if T and S are both of shape λ and have content $\{1^{e_1}, \ldots, r^{e_r}\}$, then $\psi(T) = \psi(S)$ if and only if $T = S$.

Lemma 31. *Suppose S and T are distinct column SSYT of the same shape and have the same content $\{1^{e_1}, \ldots, r^{e_r}\}$. Then $\psi(T) \neq \psi(S)$.*

Proof. Since the contents of S and T are identical, all boxes of S and T with filled with i are relabelled with some integer in the set $\{(e_1 + \ldots + e_{i-1}) + 1, \ldots, (e_1 + \ldots + e_{i-1}) + e_i\}$ by definition of the map ψ. As S and T are distinct column SSYT, there is some pair of integers j, k such that $T_{jk} = i$ and $S_{jk} = i'$ with $i \neq i'$. Then

$$\psi(T)_{jk} \in \{(e_1 + \ldots + e_{i-1}) + 1, \ldots, (e_1 + \ldots + e_{i-1}) + e_i\}$$

and

$$\psi(S)_{jk} \in \{(e_1 + \ldots + e_{i'-1}) + 1, \ldots, (e_1 + \ldots + e_{i'-1}) + e_i\}.$$

These sets are disjoint and so $\psi(T) \neq \psi(S)$. $\square$

We now shift our focus towards the promotion of SSYT. Note that the promotion operator from Section 2.1 generalizes to SSYT by performing the standard promotion once for every 1 that appears in the tableau.

Definition 32 (Promotion of SSYT)**.** Given a column SSYT T with content $\{1^{e_1}, \ldots, n^{e_n}\}$, the *promotion* of T is the column SSYT $P(T)$ with content $\{1^{e_2}, \ldots, (n-1)^{e_n}, n^{e_1}\}$ created as follows:

1. Erase 1 in the top left corner of T and leave an empty box.
2. Given the configuration $\begin{array}{|c|c|}\hline & b \\ \hline a & \\ \cline{1-1}\end{array}$ and $b \leqslant a$ then slide b left; else if $a < b$ slide a up.
3. Repeat the above process until there are no nonempty boxes below or to the right of the empty box.
4. Repeat steps (1) through (3) until all e_1 copies of 1 have been removed from the tableau.
5. Decrement all entries by 1 and insert e_1 copies of n in the empty boxes.

Since the promotion of SSYT is in essence a repeated application of promotion for SYT, it is natural to expect that the map ψ from SSYT to SYT and the promotion operator P commute in some natural way. The next result shows that this is true and characterises how the two maps interact.

Lemma 33. *Suppose T is a column SSYT with content $\{1^{e_1}, \ldots, r^{e_r}\}$. Then the promotion map commutes with the map ψ to standard Young tableaux in the following sense:*

$$\psi(P(T)) = P^{e_1}(\psi(T)).$$

Proof. We prove this by induction on e_1. When $e_1 = 1$ we compare the path of one empty box in the SSYT T and SYT $\psi(T)$ under repeated slides of the form of Step (2) in the promotion algorithm. The map ψ is defined so that if $a < b$ then the entry of every box in $\psi(T)$ that was labeled a in T is less than the entry of every box in $\psi(T)$ that was labeled b in T. This means that the empty box in Step (2) slides the same direction when promoting $\psi(T)$ as T except perhaps if $a = b$. In that case, we have the following configurations in T (on the left) and $\psi(T)$ (on the right):

$$\begin{array}{|c|c|}\hline & a \\ \hline a & \\ \cline{1-1}\end{array} \qquad\qquad \begin{array}{|c|c|}\hline & a' \\ \hline a'+1 & \\ \cline{1-1}\end{array}$$

For both tableaux, promotion's Step (2) slides the empty box to the right. Repeating, we conclude that the empty box stays in the same position after each iteration of Step (2). Thus, two things are true when we first encounter Step (4) in the promotion algorithm: first, the empty box slid along the same path and ended in the same position in T as in $\psi(T)$; and second, when $k = 1$ we know $P(\psi(T)) = \psi(P(T))$.

Now suppose $k \geqslant 2$ and take as inductive hypothesis that for any tableau T' with $e_1 = k-1$ instances of one, $P^{e_1}(\psi(T')) = P^{k-1}(\psi(T')) = \psi(P(T'))$. Now let T be a column SSYT for which one occurs $e_1 = k$ times in T. Let T' be the column SSYT obtained when we first encounter Step (4) in promoting T. By definition, we know T' is a column SSYT with $k-1$ instances of one and with $|T|-1$ boxes. Moreover, by the previous paragraph, the tableau obtained at Step (4) of promoting $\psi(T)$ has the same shape as T' and all boxes were slid in exactly the same way. In other words, the tableau at Step (4) of promoting $\psi(T)$ differs from $\psi(T')$ only by subtracting one from each entry. By induction, we know that $\psi(P(T')) = P^{k-1}(\psi(T'))$. By the previous paragraph, we know that $\psi(P(T'))$ differs from $\psi(P(T))$ only by inserting a box with the largest entry of T into the same position as the box with entry $|T|$ in $\psi(P(T))$, completing the proof. $\square$

Given a multiset $\{1^{e_1}, \ldots, r^{e_r}\}$, let R be the smallest integer such that $e_{i+R \mod (r)} = e_i$ for all $1 \leqslant i \leqslant r$. We now provide a formula to compute $|\mathcal{O}(T)|$ using $|\mathcal{O}(\psi(T))|$ and R.

Theorem 34. *Let T be a column SSYT with content $\{1^{e_1}, \ldots, r^{e_r}\}$, and let R be as above. Then $|\mathcal{O}(T)| = \ell R$ where*

$$\ell \sum_{i=1}^{R} e_i = \operatorname{lcm}\left(\sum_{i=1}^{R} e_i, |\mathcal{O}(\psi(T))|\right).$$

Proof. First observe that because $e_{i+|\mathcal{O}(T)| \mod (r)} = e_i$ for all $1 \leqslant i \leqslant r$, it follows by an argument analogous to that of Lemma 23 that $R \,|\, |\mathcal{O}(T)|$. Say $|\mathcal{O}(T)| = \ell R$.

Lemma 33 says $\psi(P(T)) = P^{e_1}(\psi(T))$. Extending this result gives $\psi(P^{\ell R}(T)) = P^t(\psi(T))$ where $t = \sum_{i=1}^{\ell R} e_{i \mod (r)}$. Observe that we can rewrite t as follows:

$$\begin{aligned} t &= \sum_{i=1}^{\ell R} e_{i \mod (r)} \\ &= \sum_{i=1}^{R} e_{i \mod (r)} + \sum_{i=R+1}^{2R} e_{i \mod (r)} + \ldots + \sum_{i=R(\ell-1)+1}^{\ell R} e_{i \mod (r)} \\ &= \ell \sum_{i=1}^{R} e_i \end{aligned}$$

Since $\psi(P^{\ell R}(T)) = \psi(T) = P^t(\psi(T))$, we see that $|\mathcal{O}(\psi(T))|$ divides t. In other words, $t = \ell \sum_{i=1}^{R} e_i$ is a multiple of $|\mathcal{O}(\psi(T))|$.

For the sake of contradiction, say there is some $0 < \ell' < \ell$ such that $\ell' \sum_{i=1}^{R} e_i$ is a multiple of $|\mathcal{O}(\psi(T))|$. Since $\ell' R < \ell R = |\mathcal{O}(T)|$, this means $P^{\ell' R}(T) \neq T$ but $P^{t'}(\psi(T)) =$

$\psi(T)$ where $t' = \ell' \sum_{i=1}^{R} e_i$. However, we know by Lemma 33, $\psi(P^{\ell' R}(T)) = P^{t'}(\psi(T))$. This means we have two distinct SSYT, T and $P^{\ell' R}(T)$, of identical shape and content mapping to the same SYT under ψ. By Lemma 31, this is not possible and so we conclude that the equality

$$\ell \sum_{i=1}^{R} e_i = \operatorname{lcm}\left(\sum_{i=1}^{R} e_i, |\mathcal{O}(\psi(T))|\right),$$

holds, thus completing the proof. $\square$

Remark 35. The formula in Theorem 34 does not require the assumption that the SSYT T is rectangular. However, if T is not rectangular, then $\psi(T)$ is also not rectangular and thus Theorem 25 cannot be applied to determine the orbit length $|\mathcal{O}(\psi(T))|$.

Example 36. We now calculate the orbit length $|\mathcal{O}(T)|$ for the tableau T in Figure 9.

The content of T is $\{1, 2, 3^4, 4, 5, 6^4, 7, 8, 9^4, 10, 11, 12^4\}$. Note that $e_{i+4 \mod 12} = e_i$ for $i = 1, \ldots, 12$ and 4 is the smallest positive integer R such that $e_{i+R \mod 12} = e_i$ for all i. Thus, the orbit length $|\mathcal{O}(T)|$ is a multiple of 4.

We now need to calculate the orbit length $|\mathcal{O}(\psi(T))|$. Since $\psi(T)$ is a rectangular SYT, we use the results of Theorem 25. First, we construct the $m-$diagram $\phi(\psi(T))$.

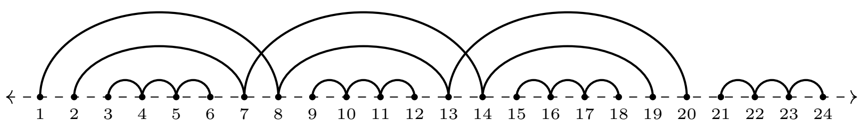

$\phi(\psi(T))$

The $m-$diagram $\phi(\psi(T))$ has 5 components C_1, C_2, C_3, C_4, C_5 with sets of endpoints

$$\begin{aligned}
\partial C_1 &= \{1, 2, 7, 8, 13, 14, 19, 20\} \\
\partial C_2 &= \{3, 4, 5, 6\} \\
\partial C_3 &= \{9, 10, 11, 12\} \\
\partial C_4 &= \{15, 16, 17, 18\} \\
\partial C_5 &= \{21, 22, 23, 24\}.
\end{aligned}$$

The minimal value of N such that $\sqcup_{i=1}^{5} \rho^N(\partial C_i) = \sqcup_{i=1}^{5} \partial C_i$ is $N = 6$ and so $\phi(\psi(T))$ has order 6 rotational symmetry. Next, since the orbit length $|\mathcal{O}(\psi(T))|$ must divide 24, we conclude $|\mathcal{O}(\psi(T))| = 6, 12$, or 24. We now evaluate the 6-fold promotions of each tableau T_{C_i} corresponding to the components C_i.

$$\begin{array}{ccccc}
\begin{array}{|c|c|}\hline 1 & 2 \\\hline 7 & 8 \\\hline 13 & 14 \\\hline 19 & 20 \\\hline\end{array} &
\begin{array}{|c|}\hline 3 \\\hline 4 \\\hline 5 \\\hline 6 \\\hline\end{array} &
\begin{array}{|c|}\hline 9 \\\hline 10 \\\hline 11 \\\hline 12 \\\hline\end{array} &
\begin{array}{|c|}\hline 15 \\\hline 16 \\\hline 17 \\\hline 18 \\\hline\end{array} &
\begin{array}{|c|}\hline 21 \\\hline 22 \\\hline 23 \\\hline 24 \\\hline\end{array} \\
T_{C_1} & T_{C_2} & T_{C_3} & T_{C_4} & T_{C_5}
\end{array}$$

Since all entries of T_{C_3}, T_{C_4} and T_{C_5} are greater than 6, we calculate the 6-fold promotion of these tableaux by subtracting 6 from each entry:

$$\underset{P^6(T_{C_3})}{\begin{array}{|c|}\hline 3\\\hline 4\\\hline 5\\\hline 6\\\hline\end{array}} \qquad \underset{P^6(T_{C_4})}{\begin{array}{|c|}\hline 9\\\hline 10\\\hline 11\\\hline 12\\\hline\end{array}} \qquad \underset{P^6(T_{C_5}).}{\begin{array}{|c|}\hline 15\\\hline 16\\\hline 17\\\hline 18\\\hline\end{array}}$$

So the equalities $P^6(T_{C_3}) = T_{C_2}, P^6(T_{C_4}) = T_{C_3}$, and $P^6(T_{C_5}) = T_{C_4}$ hold. We now calculate $P^6(T_{C_1})$ and $P^6(T_{C_2})$ using the arguments in Remark 20:

$$\underset{T_{C_1}}{\begin{array}{|c|c|}\hline 1&2\\\hline 7&8\\\hline 13&14\\\hline 19&20\\\hline\end{array}} \dashrightarrow \underset{P^2(T_{C_1})}{\begin{array}{|c|c|}\hline 5&6\\\hline 11&12\\\hline 17&28\\\hline 23&24\\\hline\end{array}} \dashrightarrow \underset{P^6(T_{C_1})}{\begin{array}{|c|c|}\hline 1&2\\\hline 7&8\\\hline 13&14\\\hline 19&20\\\hline\end{array}}$$

$$\underset{T_{C_1}}{\begin{array}{|c|}\hline 3\\\hline 4\\\hline 5\\\hline 6\\\hline\end{array}} \dashrightarrow \underset{P^2(T_{C_1})}{\begin{array}{|c|}\hline 1\\\hline 2\\\hline 3\\\hline 4\\\hline\end{array}} \dashrightarrow \underset{P^6(T_{C_1}).}{\begin{array}{|c|}\hline 21\\\hline 22\\\hline 23\\\hline 24\\\hline\end{array}}$$

So we have that $P^6(T_{C_1}) = T_{C_1}$ and $P^6(T_{C_2}) = T_{C_5}$ and thus $\mathcal{O}(\psi(T)) = 6$.

Using the notation of Theorem 34, we conclude $R = 3$ and $|\mathcal{O}(\psi(T))| = 6$. Note that $\sum_{i=1}^{R} e_i = 6$. Choosing ℓ to satisfy the equality

$$\ell \sum_{i=1}^{R} e_i = \ell \cdot 6 = \operatorname{lcm}(6, |\mathcal{O}(\psi(T))|) = \operatorname{lcm}(6, 6)$$

we see that $\ell = 1$ suffices. Thus the orbit length $|\mathcal{O}(T)| = 1 \cdot 3 = 3$.

Acknowledgements

We would like to thank Meredith Pan and Risa Vandegrift for helpful discussions during the early stages of this work. We would also like to express gratitude to anonymous reviewers for careful and thoughtful reviews of the paper. EC was partially supported by a GAANN Fellowship under Award P200A240046. HR was partially supported by an AMS-Simons Research Enhancement Grant for PUI Faculty. JT was partially supported by NSF DMS grants 1800773, 2054513, and 2349088, and an AWM MERP fellowship.

References

[1] Per Alexandersson, Stephan Pfannerer, Martin Rubey, and Joakim Uhlin. Skew characters and cyclic sieving. *Forum Math. Sigma*, 9:Paper No. e41, 31, 2021.

[2] Drew Armstrong, Christian Stump, and Hugh Thomas. A uniform bijection between nonnesting and noncrossing partitions. *Trans. Amer. Math. Soc.*, 365(8):4121–4151, 2013.

[3] Bruce Fontaine and Joel Kamnitzer. Cyclic sieving, rotation, and geometric representation theory. *Selecta Mathematica*, 20(2):609–625, 2014.

[4] William Fulton. *Young Tableaux: With Applications to Representation Theory and Geometry*. London Mathematical Society Student Texts. Cambridge University Press, 1996.

[5] Christian Gaetz, Oliver Pechenik, Stephan Pfannerer, Jessica Striker, and Joshua P Swanson. Rotation-invariant web bases from hourglass plabic graphs. *Inventiones Mathematicae*, 243(2): 703–804, 2026

[6] Mark D Haiman. Dual equivalence with applications, including a conjecture of proctor. *Discrete Mathematics*, 99(1-3):79–113, 1992.

[7] Mikhail Khovanov and Greg Kuperberg. Web bases for sl(3) are not dual canonical. *Pacific Journal of Mathematics*, 188(1): 129–153, 1999.

[8] Greg Kuperberg. Spiders for rank 2 lie algebras. *Communications in mathematical physics*, 180(1):109–151, 1996.

[9] Joseph Pappe, Stephan Pfannerer, Anne Schilling, and Mary Claire Simone. Promotion and growth diagrams for fans of Dyck paths and vacillating tableaux. *J. Algebra*, 655:794–842, 2024.

[10] Oliver Pechenik. Cyclic sieving of increasing tableaux and small Schröder paths. *J. Combin. Theory Ser. A*, 125:357–378, 2014.

[11] Oliver Pechenik and Alexander Yong. Genomic tableaux. *J. Algebraic Combin.*, 45(3):649–685, 2017.

[12] T Kyle Petersen, Pavlo Pylyavskyy, and Brendon Rhoades. Promotion and cyclic sieving via webs. *J. of Algebraic Combin.*, 30:19–41, 2009.

[13] Stephan Pfannerer, Martin Rubey, and Bruce Westbury. Promotion on oscillating and alternating tableaux and rotation of matchings and permutations. *Algebr. Comb.*, 3(1):107–141, 2020.

[14] Kevin Purbhoo and Donguk Rhee. Minimal orbits of promotion. *Electron. J. Combin.*, 24(1):Paper No. 1.41, 17, 2017.

[15] V. Reiner, D. Stanton, and D. White. The cyclic sieving phenomenon. *J. Combin. Theory Ser. A*, 108(1):17–50, 2004.

[16] Brendon Rhoades. Cyclic sieving, promotion, and representation theory. *J. Combin. Theory Ser. A*, 117(1):38–76, 2010.

[17] Heather M Russell. An explicit bijection between semi-standard tableaux and non-elliptic sl 3 webs. *Journal of Algebraic Combinatorics*, 38:851–862, 2013.

[18] Heather M Russell and Julianna Tymoczko. Stranding $\mathfrak{sl}_n$ webs. *arXiv preprint arXiv:2510.12035*, 2025.

[19] Marcel-Paul Schützenberger. Promotion des morphismes d'ensembles ordonnés. *Discrete Mathematics*, 2(1):73–94, 1972.

[20] Richard P. Stanley. *Enumerative Combinatorics*. Cambridge Studies in Advanced Mathematics. Cambridge University Press, 1999.

[21] Jessica Striker. Dynamical algebraic combinatorics: promotion, rowmotion, and resonance. *Notices Amer. Math. Soc.*, 64(6):543–549, 2017.

[22] Jessica Striker. Rowmotion and generalized toggle groups. *Discrete Math. Theor. Comput. Sci.*, 20(1):Paper No. 17, 26, 2018.

[23] Jessica Striker and Nathan Williams. Promotion and rowmotion. *European J. Combin.*, 33(8):1919–1942, 2012.

[24] Hugh Thomas and Alexander Yong. A jeu de taquin theory for increasing tableaux, with applications to K-theoretic Schubert calculus. *Algebra Number Theory*, 3(2):121–148, 2009.

[25] Hugh Thomas and Alexander Yong. Equivariant Schubert calculus and jeu de taquin. *Ann. Inst. Fourier (Grenoble)*, 68(1):275–318, 2018.

[26] Julianna Tymoczko. A simple bijection between standard $3 \times n$ tableaux and irreducible webs for $\mathfrak{sl}_3$ *Journal of Algebraic Combinatorics*, 35(4):611–632, 2012.

[27] Bruce W. Westbury/ Invariant tensors and the cyclic sieving phenomenon *Electron. J. Combin.* 23(4):Paper 4.25, 40, 2016.